

This discussion paper is/has been under review for the journal Atmospheric Chemistry and Physics (ACP). Please refer to the corresponding final paper in ACP if available.

Simulation of aerosol optical thickness during IMPACT (May 2008, The Netherlands) with ECHAM5-HAM

G.-J. Roelofs¹, H. ten Brink², A. Kiendler-Scharr³, G. de Leeuw^{4,5,6}, A. Mensah³, A. Minikin⁷, and R. Otjes²

¹Institute for Marine and Atmospheric Research Utrecht (IMAU), Utrecht University, Princetonplein 5, 3584 CC Utrecht, The Netherlands

²Energy Center Netherlands (ECN), Petten, The Netherlands

³ICG-2: Troposphere, Forschungszentrum Jülich GmbH, Germany

⁴Business unit Environment, Health and Safety, TNO, Utrecht, The Netherlands

⁵Finnish Meteorological Institute, Climate Change Unit, Helsinki, Finland

⁶University of Helsinki, Department of Physics, Helsinki, Finland

⁷Deutsches Zentrum für Luft- und Raumfahrt (DLR), Oberpfaffenhofen, Germany

Received: 27 January 2010 – Accepted: 18 February 2010 – Published: 1 March 2010

Correspondence to: G. J. H. Roelofs (g.j.h.roelofs@uu.nl)

Published by Copernicus Publications on behalf of the European Geosciences Union.

Simulation of aerosol optical thickness during IMPACT

G. J. H. Roelofs et al.

Title Page

Abstract

Introduction

Conclusions

References

Tables

Figures

◀

▶

◀

▶

Back

Close

Full Screen / Esc

Printer-friendly Version

Interactive Discussion



Abstract

In May 2008 the measurement campaign IMPACT for observation of atmospheric aerosol and cloud properties was conducted in Cabauw (The Netherlands). With a nudged version of the coupled aerosol-climate model ECHAM5-HAM we simulate aerosol and aerosol optical thickness (AOT) for the campaign period. Synoptic scale meteorology is represented realistically and simulated concentrations of aerosol sulfate and organics at the surface are generally within a factor of two from observed values. The monthly averaged AOT from the model is 0.33, about 20% larger than observed. For selected periods of the month with relatively dry and moist conditions discrepancies are approximately -30% and $+15\%$, respectively. Discrepancies during the dry period are partly caused by inaccurate representation of boundary layer (BL) dynamics by the model affecting the simulated AOT. The model simulates too strong exchange between the BL and the free troposphere, resulting in weaker concentration gradients at the BL top than observed for aerosol and humidity, while upward mixing from the surface layers into the BL appears to be underestimated. The results indicate that beside aerosol sulfate and organics also aerosol ammonium and nitrate significantly contribute to aerosol water uptake. The relation between particle concentration and AOT is rather weak during IMPACT. The simulated day-to-day variability of AOT follows synoptic scale advection of humidity rather than particle concentration. Even for relatively dry conditions AOT appears to be strongly influenced by the diurnal cycle of RH in the lower boundary layer, further enhanced by uptake and release of nitric acid and ammonia by aerosol water.

1 Introduction

Aerosol particles influence optical characteristics and the lifetime of clouds through the so-called first and second aerosol indirect effects (e.g., Lohmann and Feichter, 2005). Anthropogenic activities have caused an increase of the atmospheric burden of aerosol

ACPD

10, 5911–5945, 2010

Simulation of aerosol optical thickness during IMPACT

G. J. H. Roelofs et al.

Title Page

Abstract

Introduction

Conclusions

References

Tables

Figures

◀

▶

◀

▶

Back

Close

Full Screen / Esc

Printer-friendly Version

Interactive Discussion



and aerosol precursors compared to the pre-industrial atmosphere, and this may have altered regional and global radiative cloud forcing (e.g., Forster et al., 2007). The large spatial and temporal variability in size, chemical composition, and hygroscopicity of particles impede accurate estimation of the aerosol direct and indirect forcing (Textor et al., 2006) and lead to large uncertainties in assessing the sensitivity of climate to human perturbations and in projections of climate change (Andreae et al., 2005).

To estimate the magnitude of the radiative forcing due to aerosol direct and indirect effects, coupled aerosol-climate models that simulate activation of aerosol to cloud droplets can be applied (Lohmann et al., 2007; Penner et al., 2006). Due to the complexity of aerosol processes and inaccuracies in the representation of the hydrological cycle, current model estimates of the radiative forcing display a large range, between -0.2 and -0.9 W m^{-2} for the direct effect and between -0.5 and -1.5 W m^{-2} for the indirect effect (Forster et al., 2007; Quaas et al., 2009). Analysis of aerosol properties retrieved from satellite measurements may help to decrease current uncertainties in aerosol burden and global distribution (e.g., Kaufman et al., 2002). Retrieved aerosol optical thickness (AOT) is assumed to indicate the aerosol column burden while the Angström exponent can be used to estimate the fine fraction of the aerosol, often associated with the anthropogenic contribution (Kaufman et al., 2005; Anderson et al., 2005). Estimates of the aerosol climate forcing based on satellite retrieval are $-1.9 \pm 0.3 \text{ W m}^{-2}$ (Bellouin et al., 2005) and $-0.9 \pm 0.4 \text{ W m}^{-2}$ (Quaas et al., 2008) for the direct effect, and $-0.2 \pm 0.1 \text{ W m}^{-2}$ for the indirect effect (Quaas et al., 2008). The inconsistency between model and remote sensing estimates may be due to the model representation of aerosol and cloud processes (Quaas et al., 2009) or the uncertain influence of black carbon (Myhre et al., 2009). Other reasons are associated with relative humidity (RH). These are the non-linear swelling of hygroscopic aerosol through water uptake especially for RH larger than $\sim 80\%$ (Schuster et al., 2006), the influence of cloud processing on AOT and Angström exponent (Roelofs and Kamphuis, 2009), and the influence of RH and its sub-grid scale variability (Bian et al., 2009; Jeong et al., 2007). Nevertheless, Andreae (2009) reports a good correlation between CCN

Simulation of aerosol optical thickness during IMPACT

G. J. H. Roelofs et al.

Title Page

Abstract

Introduction

Conclusions

References

Tables

Figures

◀

▶

◀

▶

Back

Close

Full Screen / Esc

Printer-friendly Version

Interactive Discussion



concentrations and AOT values, based on observations in different air masses with varying pollution levels and particle concentrations ranging over several orders of magnitude. However, for measurements associated with relatively similar pollution levels, i.e., within an order of magnitude, the correlation appears less robust (their Fig. 1).

5 In this study we simulate atmospheric aerosol and AOT in May 2008, with a coupled aerosol-climate model, ECHAM5-HAM. The model contains a size-resolved representation of aerosol and different aerosol components, and a sophisticated aerosol activation and cloud chemistry parameterization. The purpose of the study is to validate simulated aerosol properties and AOT, and to investigate the contribution of different parameters (particle concentrations, chemical composition and RH) on the column integrated AOT. For the validation of aerosol parameters we use measurements
10 obtained during the IMPACT campaign in May 2008 (Intensive Measurement campaign at Cabauw Tower) (Cabauw, The Netherlands, 51°58' N, 4°54' E). IMPACT was conducted as part of EUCAARI, a European project aimed to reduce uncertainties associated with aerosol climate effects and to quantify the impact on climate of air quality directives in Europe. Measurements were conducted at the surface, from a
15 200 m measurement tower, with balloon sondes and from a helicopter and from aircraft. These resulted in detailed information on meteorological parameters, aerosol size-distribution and chemical composition, atmospheric trace gases, radiative fluxes and cloud parameters. For more information on EUCAARI we refer to the overview paper by Kulmala et al. (2009). For AOT we use values from the Aerosol Robotic Network (AERONET, <http://aeronet.gsfc.nasa.gov/>). AERONET is a worldwide net of ground-based remote sensing of aerosol that provides observations of spectral aerosol optical thickness (AOT) and several inversion products.

25 Section 2 of this manuscript provides a description of the coupled aerosol-climate model. Section 3 presents time series of several observed and simulated meteorological parameters and aerosol optical and chemical properties in May 2008 at Cabauw. In Sect. 4 three characteristic episodes in this month are discussed in more detail. Section 5 presents a summary of the results and conclusions.

Simulation of aerosol optical thickness during IMPACT

G. J. H. Roelofs et al.

[Title Page](#)[Abstract](#)[Introduction](#)[Conclusions](#)[References](#)[Tables](#)[Figures](#)[⏪](#)[⏩](#)[◀](#)[▶](#)[Back](#)[Close](#)[Full Screen / Esc](#)[Printer-friendly Version](#)[Interactive Discussion](#)

2 Model description

We use a version of the coupled aerosol-climate model ECHAM5-HAM similar to the one applied by Stier et al. (2005). ECHAM5-HAM consists of the general circulation model ECHAM version 5 and an aerosol module (HAM). The model uses 19 vertical layers in a hybrid σ -p-coordinate system, from the surface to 10 hPa. Average pressure levels in the troposphere are 990, 970, 950, 900, 840, 760, 670, 580, 490, 400, 320 and 250 hPa, referring to approximate mid-layer altitudes of 0.03, 0.14, 0.38, 0.78, 1.4, 2.1, 3.1, 4.2, 5.6, 7.0, 8.6 and 10.2 km above the surface, respectively. The horizontal resolution is T63 ($\sim 1.8^\circ$). The meteorology is nudged with ECMWF 6-hourly spectral re-analysis data for vorticity, divergence, temperature and surface pressure, starting from January 2008. The parameters are used by ECHAM5 to compute actual wind fields. Further, atmospheric water vapor is not nudged but follows directly from the simulation of the atmospheric hydrological cycle.

HAM accounts for emissions of aerosol and aerosol precursors, chemical transformations, nucleation of new particles and condensation of semi-volatile H_2SO_4 on existing particles, coalescence between particles and dry and wet deposition. The core of HAM is the aerosol dynamical module M7 (Vignati et al., 2004; Wilson et al., 2001). M7 describes the aerosol population with four soluble and three insoluble aerosol modes composed of (mixtures of) sulfate, organic carbon, black carbon, sea salt and dust. The modes are described as lognormal distributions of particle concentrations, and each mode is characterized by the total particle number concentration and mass of associated aerosol components. The size ranges considered are below $0.005 \mu\text{m}$ dry particle radius for the nucleation mode, between 0.005 and $0.05 \mu\text{m}$ dry particle radius for the Aitken mode, between 0.05 and $0.5 \mu\text{m}$ dry particle radius for the accumulation mode, and above $0.5 \mu\text{m}$ dry particle radius for the coarse mode. The model considers emissions of the aerosol precursor gas SO_2 and dimethyl sulfide, and calculates sulfate formation in the gaseous and aqueous phase using offline oxidant fields. All other emissions are treated as primary. Also, formation of secondary organic aerosol

Simulation of aerosol optical thickness during IMPACT

G. J. H. Roelofs et al.

Title Page

Abstract

Introduction

Conclusions

References

Tables

Figures

◀

▶

◀

▶

Back

Close

Full Screen / Esc

Printer-friendly Version

Interactive Discussion



Simulation of aerosol optical thickness during IMPACTG. J. H. Roelofs et al.

(SOA) is not calculated explicitly but all organics are emitted as primary particles. The molecular weight of oxalic acid is taken to be representative for the organic matter, and the organics are distributed evenly over the soluble and insoluble aerosol modes. The organics in the soluble aerosol are assumed to have a soluble fraction of 50% while surface tension effects are neglected. The emissions of dust, sea salt, dimethyl sulfide and marine organics are calculated online (Stier et al., 2005; Roelofs, 2008). The emissions of other aerosol compounds are based on the AEROCOM emission inventory and representative for the year 2000 (Dentener et al., 2006). In the Cabauw grid anthropogenic emissions dominate, with $1.5 \times 10^{-10} \text{ kg S m}^{-2} \text{ s}^{-1}$ and $3.0 \times 10^{-11} \text{ kg organic C m}^{-2} \text{ s}^{-1}$.

The bulk cloud chemistry scheme in ECHAM5-HAM has been replaced with a cloud processing parameterization (Roelofs et al., 2006). First, the cloud drop number concentration is estimated through an empirical approach. The second step in the parameterization calculates aqueous phase formation of sulfate and its distribution over the different activated modes, i.e., the modes that contribute to CDNC. The parameterization is linked to the climate model's large-scale cloud scheme (Lohmann and Roeckner, 1996). In the current study the cloud droplet concentration is not coupled to the calculation of precipitation formation and cloud optical properties.

North-West Europe is characterized by relatively high concentrations of nitric acid and ammonia (e.g., Myhre et al., 2006). Our model does not consider aerosol chemistry associated with nitric acid and ammonia, although a prescribed aerosol ammonium concentration results from our assumption that half of the computed sulfate amount is immediately neutralized by ammonium. We implemented a simple equilibrium dissolution and dissociation module for nitric acid, which is considered on the Cabauw grid for AOT calculations only. A HNO_3 gas phase concentration in the boundary layer of 3 ppb is prescribed, which corresponds to the sum of the observed HNO_3 and aerosol nitrate concentrations of $\sim 8 \mu\text{g}/\text{m}^3$.

The AOT calculations are based on the simulated modal masses of the individual aerosol components and the particle number concentration for each mode. These

[Title Page](#)[Abstract](#)[Introduction](#)[Conclusions](#)[References](#)[Tables](#)[Figures](#)[◀](#)[▶](#)[◀](#)[▶](#)[Back](#)[Close](#)[Full Screen / Esc](#)[Printer-friendly Version](#)[Interactive Discussion](#)

are used to calculate the median dry particle radius, and for the soluble modes also the median wet radius. In the standard model version the wet radius is calculated from the simulated aerosol sulfate and sea salt burdens (Vignati et al., 2004). In the present study we employ a more versatile approach based on the Koehler equation that considers also ammonium, nitrate, hydrogen ions and soluble organic matter.

3 Results

3.1 Meteorological and aerosol parameters

Figure 1 shows AOT and the Angström exponent from AERONET (level 1.5) at Cabauw in May 2008, and the corresponding simulation results. We transformed the measurements for 440 nm by means of the observed Angström exponent to 553 nm, the wavelength employed by ECHAM. The estimated uncertainty of AOT from AERONET is ± 0.02 (Eck et al., 2005).

The observations from May 2008 at Cabauw suggest a sequence of periods with typical AOT values. Periods with AOT exceeding 0.5 are 2–4 May, 14–16 May and May 22–31. The average observed AOT (553 nm) in May 2008 in Cabauw is 0.275. Figure 1 also shows simulation results for cloud-free conditions, i.e., the simulated grid-averaged liquid water and ice columns combined do not exceed 0.05 g/m^2 . The average simulated AOT for this threshold is 0.329, 20% larger than observed. It is highly sensitive for the cloud filter applied. For threshold values of 0.01 g/m^2 and 0.10 g/m^2 the average AOT is 0.230 and 0.396, respectively. The simulated contributions to AOT (553 nm) by the fine (Aitken and accumulation) and coarse mode fractions are 0.241 and 0.088, respectively, as compared to observed values of 0.180 and 0.095, respectively (not shown). The Angström exponent (AE) (Fig. 1b) shows considerable scatter in the first four days, these are followed by relatively high AE until 24 May indicating a relatively large fraction of fine mode particles, and relatively small values after 24 May indicating a significant coarse mode particle concentration.

Simulation of aerosol optical thickness during IMPACT

G. J. H. Roelofs et al.

Title Page

Abstract

Introduction

Conclusions

References

Tables

Figures

◀

▶

◀

▶

Back

Close

Full Screen / Esc

Printer-friendly Version

Interactive Discussion



Simulation of aerosol optical thickness during IMPACTG. J. H. Roelofs et al.

[Title Page](#)[Abstract](#)[Introduction](#)[Conclusions](#)[References](#)[Tables](#)[Figures](#)[⏪](#)[⏩](#)[◀](#)[▶](#)[Back](#)[Close](#)[Full Screen / Esc](#)[Printer-friendly Version](#)[Interactive Discussion](#)

The simulated time series of AOT and AE are qualitatively consistent with the observations. However, several discrepancies can be noticed. Between 1–6 May the model situates two relatively narrow dust filaments, remnants of a Saharan dust event that occurred in April 2008, north and south of Cabauw (not shown). Considering the relatively large AOT and highly variable AE it is possible that on 2 and 3 May one filament was detected above Cabauw by AERONET, but this is not simulated. The other filament influences the Cabauw model grid on 6 May, with an AOT larger than observed. Between 7–12 May simulated AOT is smaller than observed and does not reproduce the observed diurnal variability. Simulated AE is of the right order of magnitude between 5–9 May, and tends to increase towards 12 May rather than decrease as observed. AOT is also underestimated during 18–22 May but AE is in better agreement. Periods between 13–17 and 23–31 May are characterized by a larger RH and by cloud occurrence. The model simulates larger AOT, consistent with AERONET, although about double the observed values during 28–31 May.

The individual periods are influenced by the governing wind direction, shown in Fig. 2a, with wind coming from the southeast (2–4 May), from the east (4–12 May), from the northeast and north (13–21 May), and from the east again (22–26 May). Generally, winds coming from a direction between northeast and south advect continental polluted air to Cabauw, and winds coming from the northwest advect cleaner marine air (e.g., Khlystov et al., 1996; Kusmierczyk-Michulec et al., 2007). Between 26–31 May the weather at Cabauw is influenced by an occlusion, leading to rapid variations in wind direction and a sharp minimum in AOT in the night of 28–29 May (Fig. 1a). The minimum is simulated correctly albeit a few hours later than observed. Although the daily variability is underestimated the simulated wind direction at 10 m is generally consistent with the observations, except for 1–2 and 29–31 May.

Figure 2b displays measurements from a condensation particle counter (CPC; TSI UCPC 3786) operated by ICG-2 Jülich (<http://www.fz-juelich.de/icg-2>) (in blue). Simulated concentrations reflect the sum of Aitken and accumulation mode particle concentrations. The synoptic variability in observed and simulated concentrations appears

Simulation of aerosol optical thickness during IMPACTG. J. H. Roelofs et al.

similar. During the periods with wind from the east (May 5–12, May 22–25) observed concentrations are about twice the simulated concentration, which is partly due to the different lower size limit in the observations (3 nm diameter) and in the model (5 nm radius). The observations display daily peaks up to $\sim 20\,000\text{ cm}^{-3}$ in the morning and afternoon, likely associated with efficient photochemical new particle formation. The model qualitatively captures morning peaks but afternoon peaks are generally smaller than observed. We remark that new particle formation associated with these peaks has been observed in the residual layer as well (Wehner et al., 2010). After 25 May the model simulates a strong concentration increase associated with advection of Saharan dust, while the observations show a similar increase a few days later. The discrepancy is probably associated with the complex meteorology associated with the occlusion. The simulated integrated water vapor (I WV, Fig. 2c) agrees well with the observations, although the model regularly overestimates I WV by 10–20%.

A first comparison of the time series presented in Figs. 1 and 2 indicate that the correlation between particle concentration (Fig. 2b) and AOT (Fig. 1a) is rather weak compared with the correlation between AOT and I WV. Except for 2–4 May, the periods with relatively high AOT coincide with relatively large I WV, and periods with low AOT (on 5 May, 18–20 May, and the night of 28–29 May) coincide with small I WV. This is associated with the influence of RH, a function of water vapor concentration and temperature, on the swelling of hygroscopic aerosol particles as will be discussed later.

3.2 Aerosol trace species

Figure 3 shows the simulated total aerosol mass and observed PM_{10} (<http://www.lml.rivm.nl/meetnet>) at the surface. The simulated aerosol mass is smaller than observed for most of the month mainly because of underestimation of aerosol nitrate and ammonium as will be discussed later. The model simulates two periods where dust contributes significantly to the aerosol mass. The first event occurs around 6 May and has been discussed earlier (Fig. 1). The second and largest event occurs between 26–31 May, when Saharan dust contributes $\sim 70\%$ to the simulated aerosol mass. Uncer-

[Title Page](#)[Abstract](#)[Introduction](#)[Conclusions](#)[References](#)[Tables](#)[Figures](#)[⏪](#)[⏩](#)[◀](#)[▶](#)[Back](#)[Close](#)[Full Screen / Esc](#)[Printer-friendly Version](#)[Interactive Discussion](#)

tainties in dust emission, transport and deposition, and possible inconsistencies in the model representation of the relatively complex meteorology over NW Europe on these days may have contributed to the overestimation of aerosol mass at the surface and the overestimation of AOT.

5 Figure 4 compares simulated and observed masses of aerosol species. Blue dots refer to mass spectrometer measurements from ICG-2 Jülich (Canagaratna et al., 2007) and reflect the mass contained by particles smaller than $0.56\ \mu\text{m}$ diameter ($0.28\ \mu\text{m}$ radius). This corresponds with a subset of the fine mode aerosol in the model, with an upper size limit of $0.5\ \mu\text{m}$ radius. Canagaratna et al. (2007) mention that the lens of the
10 AMS instrument, a PM_{10} instrument, offers 100% transmission for particles in the aerodynamic diameter range of 70-500nm and 50% transmission for particles with 1000nm diameter. The green dots refer to MARGA-sizer measurements from ECN (The Netherlands; <http://www.ecn.nl>) and reflect the total (i.e., fine + coarse mode) mass of the aerosol components.

15 Figure 4a shows aerosol sulfate concentrations. The calculated order of magnitude is similar as observed, but the model severely overestimates sulfate on 16–17 and 25–28 May. 16–17 May are characterized by a northerly wind that transports cleaner air to Cabauw from the North Sea, and cloudiness. However, in the model Cabauw is located in a land grid with significant emissions of pollutants, a.o. SO_2 . These are
20 instantaneously mixed throughout the grid and then influence simulated sulfate levels regardless of wind direction. The overestimate during 25–28 May is probably related to the overestimation of the atmospheric dust burden. During its northward transport over the European continent dust interacts with gaseous and particulate pollutants. Deposition of sulfuric acid on the dust surface and coagulation with pollution aerosol
25 may explain the relatively large amounts of sulfate as well as organic matter.

Observed nitrate concentrations (Fig. 4b) range between 3 and $10\ \mu\text{g}/\text{m}^3$ with occasional peaks of $20\text{--}30\ \mu\text{g}/\text{m}^3$ in relatively moist periods (13–17 May and after 26 May). This suggests that humidity significantly affects the aerosol nitrate uptake (see Fig. 2c). Simulated concentrations of aerosol nitrate, based on an initial HNO_3 concentration of

Simulation of aerosol optical thickness during IMPACT

G. J. H. Roelofs et al.

[Title Page](#)[Abstract](#)[Introduction](#)[Conclusions](#)[References](#)[Tables](#)[Figures](#)[◀](#)[▶](#)[◀](#)[▶](#)[Back](#)[Close](#)[Full Screen / Esc](#)[Printer-friendly Version](#)[Interactive Discussion](#)

3 ppbv, are on the order of $0.7 \mu\text{g}/\text{m}^3$. This is negligible compared to the observations although during moist periods simulated aerosol nitrate reaches $3\text{--}5 \mu\text{g}/\text{m}^3$. Simulated ammonium concentrations (Fig. 4c) are about half the values observed. The simulated aerosol ammonium directly follows from our assumption that aerosol sulfate is in the form of ammonium bisulfate. The potential role of ammonium and nitrate for AOT will be discussed in more detail in Sect. 4.3.

Simulated daily variability for organic matter (Fig. 4d) is larger than observed, due to the fact that the model assumes primary emissions instead of more gradual SOA formation from precursor gases. Nevertheless, on average simulated and observed concentrations agree relatively well. For chloride, which is almost exclusively found in the coarse mode, modeled peak concentrations are relatively large compared to the observations. However, both observations and model indicate that the chloride fraction in the aerosol is relatively small during most of the month (Fig. 4e). We remark that observed chloride concentrations are correlated relatively well with sodium in a mass concentration ratio of ~ 1.5 , indicating that chloride is associated with sea salt.

Figure 5 shows simulated and observed particle concentration profiles, averaged over 1–14 May. Simulated values pertain to the Cabauw grid sampled between 10.00 and 18.00, while the observations reflect aircraft measurements of 10 flights of the DLR Falcon over The Netherlands, Britain and Germany during the same period. These aircraft measurements were part of the EUCAARI-LONGREX campaign conducted during the EUCAARI Intensive Observation Period in 2008. The observed aerosol number concentration profiles in Fig. 5 are based on median values calculated for altitude bins of 800 m, for cloud-free conditions only. Data are based on measurements with a condensation particle counter and two optical aerosol spectrometer probes, a PCASP-100X and a FSSP-300. This instrument configuration is described in more detail by Weinzierl et al. (2009) and Minikin et al. (2003). Although measurements and model consider different modal size ranges, the agreement is relatively good for the accumulation and coarse modes. The measurements show a rather sharp concentration gradient for all modes between 2000 and 3000 m. Simulated gradients are weaker for

Simulation of aerosol optical thickness during IMPACT

G. J. H. Roelofs et al.

Title Page

Abstract

Introduction

Conclusions

References

Tables

Figures

◀

▶

◀

▶

Back

Close

Full Screen / Esc

Printer-friendly Version

Interactive Discussion



the accumulation and coarse modes, and not represented at all for the Aitken mode. The relatively coarse vertical resolution around this altitude (~750 m) probably contributes to the spurious mixing of aerosol and its precursors between the BL and the free troposphere.

4 Aerosol, humidity and AOT in selected periods

For a better understanding of the contribution of aerosol properties and RH to AOT three periods are examined in more detail, i.e., the relatively dry episode between 7–12 May, the moist episode between 22–26 May and the dust event between 27–30 May. Table 1 shows the average AERONET and simulated AOT for these periods, and the simulated contributions from the soluble and insoluble accumulation and coarse modes. Simulated values are filtered for clouds as explained in Sect. 3.1. The model underestimates AOT in the dry period by 30%, and overestimates AOT in the moist period by 15% and in the dust period by 80%. For the moist and dust periods the simulated AOT is again highly sensitive for the cloud filter applied. For cloud column thresholds 0.01 and 0.10 g/m², the simulated average AOT for the moist period are 0.41 and 0.56, and for the dust period 0.86 and 1.15, respectively. AOT is dominated by the contribution from the soluble accumulation mode in the dry and moist periods. In the dust period the soluble and insoluble coarse modes contribute about 70% of the AOT, which is also expressed in a relatively small AE (Fig. 1b). The simulated Aitken mode contribution to AOT is negligible.

The three periods are further compared in Fig. 6 with time-averaged profiles for particle number concentrations, sulfate, RH the accumulation mode median wet radius, the scattering coefficient μ_s (defined as the optical thickness per unit length) and the normalized cumulative (surface-to-TOA) AOT for cloud-free conditions. Simulated Aitken mode particle concentrations are similar for the three periods, about $3500 \pm 500 \text{ cm}^{-3}$ at the surface to $1500 \pm 500 \text{ cm}^{-3}$ above 500 m (Fig. 6a), reflecting continuous emissions of primary particles and precursor gases in the Cabauw grid. Accumulation mode con-

Simulation of aerosol optical thickness during IMPACT

G. J. H. Roelofs et al.

Title Page

Abstract

Introduction

Conclusions

References

Tables

Figures

◀

▶

◀

▶

Back

Close

Full Screen / Esc

Printer-friendly Version

Interactive Discussion



centrations are also similar, except for a local maximum at ~ 2200 m during the moist period which is associated with synoptic scale advection of pollution (Fig. 6b). Surface particle concentrations maximize in the dry period. Coarse mode concentrations are relatively small in the dry and moist periods, and large during the dust period (cf. Table 1), maximizing between 2 and 6 km altitude (Fig. 6c).

Aerosol sulfate concentrations are relatively small in the dry period (Fig. 6d). In the moist period sulfate maximizes at 2200 m altitude coinciding with the maximum in the accumulation mode particle concentration and humidity. This sulfate originates mostly from in-cloud sulfate formation. In the dust period aerosol sulfate is mainly associated with deposition of sulfuric acid on dust particles below 3000 m in the polluted European troposphere.

Sonde measurements of temperature and humidity at Cabauw were performed in the morning, at noon and in the late afternoon. Figure 6e shows the observed RH profiles as well as simulated daytime averaged RH profiles. The observed standard deviation of RH in the BL is approximately 0.09, 0.2 and 0.15 for the dry, moist and dust periods, respectively. In the dry period simulated RH ranges from 0.55 at the surface to 0.4 at 2000 m. RH during the moist period is higher, up to ~ 0.95 at 2000 m. Simulated RH profiles are qualitatively similar to the observations. In the dry period the simulated surface RH is larger than observed. Also, in the dry and the moist periods the model simulates a sharp inversion of RH at ~ 400 m altitude that is not observed. This may indicate that mixing between the surface layer and the rest of the boundary layer is insufficient in the model. Additionally, the observed RH gradient at the top of the BL is sharper than in the model. This indicates that the simulated mixing between the BL and the free troposphere is more efficient than in reality, which may also have resulted in the overestimation of the water vapor column (Fig. 2c). Similar discrepancies are seen in the simulated Aitken and accumulation mode concentration profiles (Fig. 5).

In the moist period simulated RH below 1500 m altitude is somewhat smaller than observed, but above 2000 m altitude it is consistently larger. At 2000 m the average observed RH is $\sim 80\%$ but simulated RH is 90% and incidentally reaches 100%. The

Simulation of aerosol optical thickness during IMPACT

G. J. H. Roelofs et al.

Title Page

Abstract

Introduction

Conclusions

References

Tables

Figures

◀

▶

◀

▶

Back

Close

Full Screen / Esc

Printer-friendly Version

Interactive Discussion



discrepancy may be partly due to sub-grid scale variability of RH (Bian et al., 2009). Aerosol swelling strongly increases with increasing RH for RH >90%, so the overestimation may have contributed to the overestimation of AOT (Table 1). In the dust period simulated RH at the surface is relatively high, 0.8, and decreases to ~0.6 in the dust plume at 3000 m. RH is smaller than observed especially at this altitude, which may be a result of inaccurate mixing between dusty and clear air masses at the edges of the dust plume.

Influenced by RH and particulate sulfate, the median wet radius of the accumulation mode (Fig. 6f) is larger in the moist and dust periods than in the dry period. Figure 6g shows the simulated scattering coefficient μ_s . Absorption in the simulation is of minor importance and will be neglected here. The scattering coefficient μ_s maximizes in the moist period, 0.25 km^{-1} at ~2000 m. During the dust period also insoluble modes and the coarse mode contribute to μ_s (see Table 2) and large values are calculated close to the surface and above 2000 m. Total attenuated backscatter measurements from CALIPSO (CloudSat, <http://www-calipso.larc.nasa.gov>) that passed Cabauw in this period at a distance of ~200 km, show that the aerosol resides predominantly below ~2 km in the dry and moist periods and below ~7 km in the dust period, consistent with our simulation. Integrating μ_s from the surface upward and dividing by AOT yields a normalized cumulative AOT profile (Fig. 6h). The profiles show that meteorological conditions strongly influence the contribution of aerosol from different tropospheric altitudes to the column AOT. In the dry period the column AOT is dominated by the BL. About 60% of AOT is contributed by aerosol residing between 250 and 2000 m, with the remainder equally divided above and below. Similarly, in the moist period 60% of the AOT derives from aerosol residing between 1500 and 2500 m where RH exceeds 90%. On average, the contribution of the boundary layer below 2000 m, where most anthropogenic aerosol resides, is ~80% for the dry period, ~60% for the moist period and ~20% for the dust period.

Simulation of aerosol optical thickness during IMPACT

G. J. H. Roelofs et al.

Title Page

Abstract

Introduction

Conclusions

References

Tables

Figures

◀

▶

◀

▶

Back

Close

Full Screen / Esc

Printer-friendly Version

Interactive Discussion



4.1 Dry period, 7–12 May

In the dry period, observed AOT ranges between 0.1 and 0.4 (Fig. 1a). On 7 and 8 May AOT minimizes at noon, and on 9–11 May AOT is increasing throughout the day. Simulated AOT is smaller than observed and does not display a distinct diurnal variability. To better understand the discrepancies between model and observations we examine the simulated fine mode particle concentration N_f , RH, the median wet radius of the accumulation mode r , and the scattering coefficient μ_s in the lower troposphere between 7–12 May (Fig. 7). Below 500 m the model simulates a relatively strong daily variability for N_f (Fig. 7a). In the morning as the intensity of sunlight and photochemical activity increases, particle concentrations increase due to new particle formation, in qualitative agreement with observed particle concentrations at the surface (Fig. 2b). The concentration decreases again after a few hours as result of the lifting of the boundary layer top, and dry convective transport carries particles upward to ~ 1800 m. A second concentration maximum at the surface occurs around 20.00 h.

RH at the surface increases during the night to $\sim 75\%$, it decreases again during the morning to 40% and increases again in the evening (Fig. 7b). At the surface r has a daily cycle varying between 65 nm and 95 nm (Fig. 7c). According to Fig. 4a the simulated sulfate burden varies less than 20%, and therefore we conclude that the variability in r is dominated by RH. The relatively strong contribution by humidity in early morning is probably a contributing factor to the finding of Schaap et al. (2009) that the correlation between AERONET AOT (reflecting both dry aerosol matter and aerosol water) and surface $PM_{2.5}$ (reflecting only dry matter) is better at noon than in the morning. A weaker daily RH cycle similar pattern is simulated in the relatively humid layer between 1200 and 1800 m, indicating that the model mixes the moisture throughout the boundary layer, but in addition synoptic scale variability causes a decrease between 7–10 May and a subsequent increase. Large values of μ_s associated with relatively large RH are simulated in the upper boundary layer above 1000 m on 7 May and above 1500 m on 12 May. Here, μ_s appears to be correlated with r (and therefore RH) rather than

Simulation of aerosol optical thickness during IMPACT

G. J. H. Roelofs et al.

Title Page

Abstract

Introduction

Conclusions

References

Tables

Figures

◀

▶

◀

▶

Back

Close

Full Screen / Esc

Printer-friendly Version

Interactive Discussion



Simulation of aerosol optical thickness during IMPACTG. J. H. Roelofs et al.

with N_f (Fig. 7d). Values of μ_s in the lowest 400 m of the BL maximize in the morning associated with peaking number concentration and RH. μ_s decreases rapidly towards noon and increases again in the early evening. The simulated behavior below 400 m mimics the variability in AOT observed by AERONET. However, the model atmosphere below 400 m contributes only about 20% to the total simulated AOT (Fig. 6h), while comparison of simulated and observed RH and particle concentration profiles indicate that the model underestimates upward mixing from the surface. A more efficient mixing, through turbulence or dry convection, will improve simulated particle concentration and RH profiles and yield a column AOT in better agreement with the observations.

4.2 Moist and dust periods, 22–30 May

Relatively few measurements are available for 25–27 May due to occurrence of clouds and precipitation. Observed AOT varies between 0.2 and 1.4 (Fig. 1a). Simulated AOT agrees reasonably well with AERONET between 23–26 May, but exceeds AERONET values after 27 May due to overestimation of the atmospheric dust burden (see Fig. 3).

Figure 8 shows fine mode particle concentration N_f , RH, r and μ_s for 22–30 May. On 22–24 May particle concentrations below 400 m altitude show a qualitatively similar pattern as in the dry period. High concentrations are simulated between 1800 and 2500 m altitude. We remark that, on average, particle concentrations are of the same order of magnitude as in the dry period in the simulation as well as observed. However, Table 1 shows that simulated (observed) AOT in the moist period is larger by a factor of 3.5 (2.2) than in the dry period. This difference is due to RH. Although the lower BL is relatively dry (Fig. 8b), in the night of 22–23 May clouds occurred in the upper BL. Clouds were also present in the night of May 24, and precipitating clouds the following days, so that on 25 May a large fraction of fine mode particles is washed out from the upper BL. The median wet radius (Fig. 8c) and μ_s again correlate well with RH, and μ_s is considerably larger than in the dry period. During 27 May the air above 400 m becomes relatively dry and fine mode particle concentrations over Cabauw decrease considerably as Saharan dust is advected. The period 27–30 May is influenced by more

[Title Page](#)[Abstract](#)[Introduction](#)[Conclusions](#)[References](#)[Tables](#)[Figures](#)[◀](#)[▶](#)[◀](#)[▶](#)[Back](#)[Close](#)[Full Screen / Esc](#)[Printer-friendly Version](#)[Interactive Discussion](#)

complicated meteorology and brings a brief intermezzo of moister, relatively clean and dustless air from Atlantic origin in the second half of May 28, leading to a minimum AOT in the night of May 28.

4.3 Sensitivity study

5 The observations indicate that the aerosol contains more than sufficient ammonium to completely neutralize sulfate. To investigate the potential influence of ammonium and nitrate on AOT we performed an additional simulation in which a ten-fold efficiency of dissolution of nitrate is assumed (see Sect. 2), and aerosol ammonium is scaled accordingly. Figure 9 shows that with this assumption the simulated concentrations and
10 diurnal cycle of nitrate and ammonium are approximately consistent with observations from ICG-2 Jülich in the dry period. A similar daily aerosol nitrate cycle and good correlation with RH has been observed in an urban background location near London (UK) (Dall'Osto et al., 2009; their Fig. 6).

The uptake of nitric acid and ammonia by the particles enhances their hygroscopicity, and this leads to additional water uptake. In the dry period when RH maximizes in the night the wet accumulation mode radius reaches ~ 110 nm, significantly larger than 95 nm simulated in the base case simulation (see Sect. 4.1). As a result, the average AOT in this period increases from 0.132 to 0.150 (+14%). The effect is stronger on relatively humid days. For example, in the morning of 27 May the simulated wet
15 accumulation mode radius at the surface is ~ 275 nm compared to 180 nm in the base case simulation. In the moist period the computed AOT increases on average from 0.469 to 0.602 (+30%). On the other hand in the dust period when insoluble aerosol is abundant AOT increases only mildly as result of the uptake, from 0.909 to 0.914 (+0.5%). The results from this sensitivity study are corroborated by simulations with
25 a column aerosol-cloud model with explicit inorganic chemistry (Derksen and Roelofs, 2010), and they suggest that RH influences AOT in various ways, not only directly via aerosol water but also indirectly through a positive feedback between the amount of aerosol water and the uptake of nitric acid and ammonia from the gas phase. We re-

Simulation of aerosol optical thickness during IMPACT

G. J. H. Roelofs et al.

Title Page

Abstract

Introduction

Conclusions

References

Tables

Figures

◀

▶

◀

▶

Back

Close

Full Screen / Esc

Printer-friendly Version

Interactive Discussion



mark that in a sensitivity simulation with an organic solubility of 10% instead of 50%, the amount of aerosol water was significantly smaller than in the base case, while AOT was smaller by approximately 14% both in the dry and in the moist period. The effect on the aerosol wet size suggests that the solubility of the aerosol organic matter can thus influence the aerosol uptake of nitric acid and ammonia, as suggested by Ming and Russell (2004).

5 Summary and discussion

We use the coupled aerosol-climate model ECHAM5-HAM, extended with a cloud activation and cloud chemistry scheme, in a nudged version to simulate the evolution of aerosol chemical and optical properties during the intensive aerosol-cloud measurement campaign IMPACT at Cabauw (The Netherlands) in May 2008. The observation period consists of a series of relatively dry and moist periods and concludes with several days characterized by advection of Saharan dust. The meteorology is represented adequately on synoptic scale, but the wind direction shows some discrepancies compared to observations while simulated IWV is larger than observed by 10–20%. The total simulated aerosol mass at the surface is about half the observed PM_{10} during most of the month, mainly due to neglect of explicit nitric acid and ammonia chemistry in the model. The dust burden over Cabauw after 25 May is overestimated. Simulated particle concentrations and concentrations of aerosol sulfate and organics are of the same order of magnitude as observed at the surface although relatively large discrepancies, up to a factor of three, occur during relatively humid conditions.

Monthly averaged values of simulated AOT are consistent within 20% with AERONET measurements. Monthly averaged AOT, however, is not a good measure of model performance since AOT displays a relatively large variability on both synoptic and hourly/diurnal scales. The model underpredicts AOT by ~30% when the atmosphere is relatively dry, and overpredicts AOT by ~15% under relatively moist conditions. Discrepancies between simulated and observed moisture and particle con-

Simulation of aerosol optical thickness during IMPACT

G. J. H. Roelofs et al.

Title Page

Abstract

Introduction

Conclusions

References

Tables

Figures

◀

▶

◀

▶

Back

Close

Full Screen / Esc

Printer-friendly Version

Interactive Discussion



centration profiles suggest that inadequate BL mixing may be partly responsible. In the dry period the upward mixing during daytime of aerosol and humidity from the surface appears too weak. Further, the transport of aerosol, aerosol precursors and humidity from the upper BL to the free troposphere appears to be overestimated. This may have caused the overestimation of the water vapor column during relatively moist days as well as the discrepancies between Aitken mode particles in the BL and the free troposphere. Nevertheless, simulated profiles of accumulation and coarse mode particle concentrations are relatively consistent with the observations. It may be expected that with a more realistic representation of BL dynamics with a less permeable BL top and realistic vertical mixing within the BL, the diurnal cycle of RH and particle concentrations will probably be expressed more prominently in AOT.

We analyzed and compared days with relatively dry and moist conditions, with a simulated AOT of 0.13 and 0.47, respectively. Aerosol dry mass and particle concentrations are of comparable magnitude in both periods, but nevertheless AOT differs by a factor of 2.2 in the observations, or 3.5 in the model. Further, the relative contribution of different atmospheric altitudes to AOT depends on the vertical distribution of RH. In the moist period the humid upper BL between 1500 and 2500 m altitude contributes relatively strongly to AOT while in the dry period the contribution is distributed more or less evenly below 2500 m altitude. This strongly suggests that RH was a dominant driver for AOT variability on synoptic scales during IMPACT, more than particle concentration and chemical composition. However, RH influences the wet particle size and AOT not only directly. In the northwest European region nitric acid and ammonia concentrations are relatively high. A simulation with realistic concentrations of aerosol ammonium and nitrate demonstrates the interplay between the RH diurnal variability and gas-aerosol cycling of ammonia and nitric acid. The enhanced water uptake leads to higher AOT, in our study up to 30%. Aerosol organic matter co-determines the aerosol water uptake to a significant extent, and thus may further influence the uptake of ammonia and nitric acid. Consequently, realistic representation in climate models of the relation between RH, aerosol inorganic and organic soluble components, water uptake and gas-aerosol

Simulation of aerosol optical thickness during IMPACT

G. J. H. Roelofs et al.

Title Page

Abstract

Introduction

Conclusions

References

Tables

Figures

◀

▶

◀

▶

Back

Close

Full Screen / Esc

Printer-friendly Version

Interactive Discussion



cycling of nitric acid and ammonia is required for accurate computation of AOT in the northwest European region.

Acknowledgements. We thank Sebastian Rast from the Max Planck Institute for Meteorology in Hamburg for his help with the nudging procedure. We thank SARA Reken- en Netwerkdiensten in Amsterdam for use of their supercomputer, and acknowledge the use of the Ferret program for the graphics (www.ferret.noaa.gov). We acknowledge AERONET for use of their data and their effort in establishing and maintaining the Cabauw site. This work has been partly funded by EUCAARI (European Integrated project on Aerosol Cloud Climate and Air Quality interactions) No 036833-2.

References

- Anderson, T. L., Wu, Y., Chu, D. A., Schmid, B., Redemann, J., and Dubovik, O.: Testing the MODIS satellite retrieval of aerosol fine-mode fraction, *J. Geophys. Res.*, 110, D18204, doi:10.1029/2005JD005978, 2005.
- Andreae, M. O., Jones, C. D., and Cox, P. M.: Strong present-day cooling implies a hot future, *Nature*, 435, doi:10.1038/nature03671, 2005.
- Andreae, M. O.: Correlation between cloud condensation nuclei concentration and aerosol optical thickness in remote and polluted regions, *Atmos. Chem. Phys.*, 9, 543–556, 2009, <http://www.atmos-chem-phys.net/9/543/2009/>.
- Bellouin, N., Boucher, O., Haywood, J., and Reddy, M. S.: Global estimate of aerosol direct radiative forcing from satellite measurements, *Nature*, 438, 1138–1141, doi:10.1038/nature04348, 2005.
- Bian, H., Chin, M., Rodriguez, J. M., Yu, H., Penner, J. E., and Strahan, S.: Sensitivity of aerosol optical thickness and aerosol direct radiative effect to relative humidity, *Atmos. Chem. Phys.*, 9, 2375–2386, 2009, <http://www.atmos-chem-phys.net/9/2375/2009/>.
- Canagaratna, M. R., Jayne, J. T., Jimenez, J. L., Allan, J. D., Alfarra, M. R., Zhang, Q., Onasch, T. B., Drewnick, F., Coe, H., Middlebrook, A., Delia, A., Williams, L. R., Trimborn, A. M., Northway, M. J., DeCarlo, P. F., Kolb, C. E., Davidovits, P., and Worsnop, D. R.: Chemical and microphysical characterization of ambient aerosols with the aerodyne aerosol mass spectrometer, *Mass Spectrom. Rev.*, 26, 185–222, 2007.

Simulation of aerosol optical thickness during IMPACT

G. J. H. Roelofs et al.

Title Page

Abstract

Introduction

Conclusions

References

Tables

Figures

◀

▶

◀

▶

Back

Close

Full Screen / Esc

Printer-friendly Version

Interactive Discussion



Simulation of aerosol optical thickness during IMPACT

G. J. H. Roelofs et al.

[Title Page](#)[Abstract](#)[Introduction](#)[Conclusions](#)[References](#)[Tables](#)[Figures](#)[◀](#)[▶](#)[◀](#)[▶](#)[Back](#)[Close](#)[Full Screen / Esc](#)[Printer-friendly Version](#)[Interactive Discussion](#)

Dall'Osto, M., Harrison, R. M., Coe, H., Williams, P. I., and Allan, J. D.: Real time chemical characterization of local and regional nitrate aerosols, *Atmos. Chem. Phys.*, 9, 3709–3720, 2009, <http://www.atmos-chem-phys.net/9/3709/2009/>.

Dentener, F., Kinne, S., Bond, T., Boucher, O., Cofala, J., Generoso, S., Ginoux, P., Gong, S., Hoelzemann, J., Ito, A., Marelli, L., Penner, J., Putaud, J.-P., Textor, C., Schulz, M., Werf, G. v. d., and Wilson, J.: Emissions of primary aerosol and precursor gases in the years 2000 and 1750 – prescribed data-sets for AeroCom, *Atmos. Chem. Phys.*, 6, 4321–4344, 2006, <http://www.atmos-chem-phys.net/6/4321/2006/>.

Eck, T. F., Holben, B. N., Dubovik, O., Smirnov, A., Goloub, P., Chen, H. B., Chatenet, B., Gomes, L., Zhang, X. Y., Tsay, S. C., Ji, Q., Giles, D., and Slutsker, I.: Columnar aerosol optical properties at AERONET sites in central eastern Asia and aerosol transport to the tropical mid-Pacific, *J. Geophys. Res.*, 110, D06202, doi:10.1029/2004JD005274, 2005.

Forster, P., Ramaswamy, V., Artaxo, P., Bernsten, T., Betts, R., Fahey, D. W., Haywood, J., Lean, J., Lowe, D. C., Myhre, G., Nganga, J., Prinn, R., Raga, G., Schulz, M., and van Dorland, R.: Changes in Atmospheric Constituents and in Radiative Forcing. In: *Climate Change 2007: The Physical Science Basis. Contribution of WG I to the Fourth Assessment Report of the Intergovernmental Panel on Climate Change*, edited by: Solomon, S., Qin, D., Manning, M., Chen, Z., Marquis, M., Averyt, K. B., Tignor, M., and Miller, H. L., Cambridge University Press, Cambridge, UK and New York, NY, USA, 2007.

Jeong, M. J., Li, Z., Andrews, E., and Tsay, S.-C.: Effect of aerosol humidification on the column aerosol optical thickness over the Atmospheric Radiation Measurement Southern Great Plains site, *J. Geophys. Res.*, 112, D10202, doi:10.1029/2006JD007176, 2007.

Kaufman, Y. J., Tanré, D., and Boucher, O.: A satellite view of aerosols in the climate system, *Nature*, 419, 215–223, 2002.

Kaufman, Y. J., Boucher, O., Tanré, D., Chin, M., Remer, L. A., and Takemura, T.: Aerosol anthropogenic component estimated from satellite data, *Geophys. Res. Lett.*, 32, L17804, doi:10.1029/2005GL023125, 2005.

Khlystov A., Kos, G. P. A., ten Brink, H. M., Kruisz, C., and Berner, A.: Activation properties of ambient aerosol in The Netherlands, *Atmos. Environ.*, 30, 3281–3290, 1996.

Kulmala, M., Asmi, A., Lappalainen, H. K., Carslaw, K. S., Pöschl, U., Baltensperger, U., Hov, Ø., Brenquier, J.-L., Pandis, S. N., Facchini, M. C., Hansson, H.-C., Wiedensohler, A., and O'Dowd, C. D.: Introduction: European Integrated Project on Aerosol Cloud Climate and Air Quality interactions (EUCAARI) – integrating aerosol research from nano to global scales,

**Simulation of aerosol
optical thickness
during IMPACT**

G. J. H. Roelofs et al.

Title Page

Abstract

Introduction

Conclusions

References

Tables

Figures

◀

▶

◀

▶

Back

Close

Full Screen / Esc

Printer-friendly Version

Interactive Discussion



- Atmos. Chem. Phys., 9, 2825–2841, 2009, <http://www.atmos-chem-phys.net/9/2825/2009/>.
- Kusmierczyk-Michulec, J., De Leeuw, G., and Moerman, M. M.: Physical and optical aerosol properties at the Dutch North Sea coast based on AERONET observations, *Atmos. Chem. Phys.*, 7, 3481–3495, 2007, <http://www.atmos-chem-phys.net/7/3481/2007/>.
- 5 Lohmann, U. and Roeckner, E.: Design and performance of a new cloud microphysics scheme developed for the ECHAM4 general circulation model, *Clim. Dyn.*, 12, 557–572, 1996.
- Lohmann, U. and Feichter, J.: Global indirect aerosol effects: a review, *Atmos. Chem. Phys.*, 5, 715–737, 2005, <http://www.atmos-chem-phys.net/5/715/2005/>.
- Lohmann, U., Quaas, J., Kinne, S., and Feichter, J.: Different approaches for constraining
10 global climate models of the anthropogenic indirect aerosol effect, *Bull. Amer. Meteor. Soc.*, 88, doi:10.1175/BAMS-88-2-243, 243–249, 2007.
- Ming, Y., and Russell, L. M.: Organic aerosol effects on fog droplet spectra, *J. Geophys. Res.*, 109, D10206, doi:10.1029/2003JD004427, 2004.
- Minikin, A., Petzold, A., Ström, J., Krejci, R., Seifert, M., Schlager, H., van Velthoven, P., and
15 Schumann, U.: Aircraft observations of the upper tropospheric fine particle aerosol in the northern and southern hemispheres at midlatitudes, *Geophys. Res. Lett.*, 30(10), 1503, doi:10.1029/2002GL016458, 2003.
- Myhre, G., Grini, A., and Metzger, S., Modelling of nitrate and ammonium-containing aerosols in presence of sea salt, *Atmos. Chem. Phys.*, 6, 4809–4821, 2006,
20 <http://www.atmos-chem-phys.net/6/4809/2006/>.
- Myhre, G.: Consistency between satellite-derived and modeled estimates of the direct aerosol effect, *Science*, 325, 187–190, doi:10.1126/science.1174461, 2009.
- Penner, J. E., Quaas, J., Storelvmo, T., Takemura, T., Boucher, O., Guo, H., Kirkevåg, A.,
Kristjánsson, J. E., and Seland, Ø.: Model intercomparison of indirect aerosol effects, *Atmos.*
25 *Chem. Phys.*, 6, 3391–3405, 2006, <http://www.atmos-chem-phys.net/6/3391/2006/>.
- Quaas, J., Boucher, O., Bellouin, N., and Kinne, S.: Satellite-based estimate of the direct and indirect aerosol climate forcing, *J. Geophys. Res.*, 113, D05204, doi:10.1029/2007JD008962, 2008.
- 30 Quaas, J., Ming, Y., Menon, S., Takemura, T., Wang, M., Penner, J. E., Gettelman, A., Lohmann, U., Bellouin, N., Boucher, O., Sayer, A. M., Thomas, G. E., McComiskey, A., Feingold, G., Hoose, C., Kristjánsson, J. E., Liu, X., Balkanski, Y., Donner, L. J., Ginoux, P. A., Stier, P., Grandey, B., Feichter, J., Sednev, I., Bauer, S. E., Koch, D., Grainger, R. G., Kirkevåg, A., Iversen, T., Seland, Ø., Easter, R., Ghan, S. J., Rasch, P. J., Morrison, H., Lamarque,

Simulation of aerosol optical thickness during IMPACT

G. J. H. Roelofs et al.

Title Page

Abstract

Introduction

Conclusions

References

Tables

Figures

◀

▶

◀

▶

Back

Close

Full Screen / Esc

Printer-friendly Version

Interactive Discussion

J.-F., Iacono, M. J., Kinne, S., and Schulz, M.: Aerosol indirect effects general circulation model intercomparison and evaluation with satellite data, *Atmos. Chem. Phys.*, 9, 8697–8717, 2009, <http://www.atmos-chem-phys.net/9/8697/2009/>.

Roelofs, G. J., Stier, P., Feichter, J., Vignati, E., and Wilson, J.: Aerosol activation and cloud processing in the global aerosol-climate model ECHAM5-HAM, *Atmos. Chem. Phys.*, 6, 2389–2399, 2006, <http://www.atmos-chem-phys.net/6/2389/2006/>.

Roelofs, G. J.: A GCM study of organic matter in marine aerosol and its potential contribution to cloud drop activation, *Atmos. Chem. Phys.*, 8, 709–719, 2008, <http://www.atmos-chem-phys.net/8/709/2008/>.

Roelofs, G. J. and Kamphuis, V.: Cloud processing, cloud evaporation and Angström exponent, *Atmos. Chem. Phys.*, 9, 71–80, 2009, <http://www.atmos-chem-phys.net/9/71/2009/>.

Schaap, M., Apituley, A., Timmermans, R. M. A., Koelemeijer, R. B. A., and de Leeuw, G.: Exploring the relation between aerosol optical depth and PM_{2.5} at Cabauw, the Netherlands, *Atmos. Chem. Phys.*, 9, 909–925, 2009, <http://www.atmos-chem-phys.net/9/909/2009/>.

Schuster, G. L., Dubovik, O., and Holben, B. N.: Angström exponent and bimodal aerosol size distributions, *J. Geophys. Res.*, 111, D07207, doi:10.1029/2005JD006328, 2006.

Stier, P., Feichter, J., Kinne, S., Kloster, S., Vignati, E., Wilson, J., Ganzeveld, L., Tegen, I., Werner, M., Balkanski, Y., Schulz, M., and Boucher, O.: The aerosol-climate model ECHAM5-HAM, *Atmos. Chem. Phys.*, 1125–1156, 2005.

Textor, C., Schulz, M., Guibert, S., Kinne, S., Balkanski, Y., Bauer, S., Berntsen, T., Berglen, T., Boucher, O., Chin, M., Dentener, F., Diehl, T., Easter, R., Feichter, H., Fillmore, D., Ghan, S., Ginoux, P., Gong, S., Grini, A., Hendricks, J., Horowitz, L., Huang, P., Isaksen, I., Iversen, I., Kloster, S., Koch, D., Kirkevåg, A., Kristjansson, J. E., Krol, M., Lauer, A., Lamarque, J. F., Liu, X., Montanaro, V., Myhre, G., Penner, J., Pitari, G., Reddy, S., Seland, Ø., Stier, P., Takemura, T., and Tie, X.: Analysis and quantification of the diversities of aerosol life cycles within AeroCom, *Atmos. Chem. Phys.*, 6, 1777–1813, 2006, <http://www.atmos-chem-phys-discuss.net/6/1777/2006/>.

Vignati, E., Wilson, J., and Stier, P.: M7: An efficient size-resolved aerosol microphysics module for large-scale aerosol transport models, *J. Geophys. Res.*, 109, D22202, doi:10.1029/2003JD004485, 2004.

Wehner, B., Siebert, H., Ansmann, A., Ditas, F., Seifert, P., Stratmann, F., Wiedensohler, A., Apituley, A., Shaw, R. A., Manninen, H. E., and Kulmala, M.: Observations of turbulence-induced new particle formation in the residual layer, *Atmos. Chem. Phys. Discuss.*, 10, 327–



360, 2010, <http://www.atmos-chem-phys-discuss.net/10/327/2010/>.

Weinzierl, B., Petzold, A., Esselborn, M., Wirth, M., Rasp, K., Kandler, K., Schütz, L., Koepke, P., and Fiebig, M.: Airborne measurements of dust layer properties, particle size distribution and mixing state of Saharan dust during SAMUM 2006, *Tellus B – Chemical and Physical Meteorology*, in press, 2009.

5 Wilson, J., Cuvelier, C., and Raes, F.: A modeling study of global mixed aerosol fields, *J. Geophys. Res.*, 106, 34081–34108, 2001.

ACPD

10, 5911–5945, 2010

Simulation of aerosol optical thickness during IMPACT

G. J. H. Roelofs et al.

Title Page

Abstract

Introduction

Conclusions

References

Tables

Figures

◀

▶

◀

▶

Back

Close

Full Screen / Esc

Printer-friendly Version

Interactive Discussion



Simulation of aerosol optical thickness during IMPACT

G. J. H. Roelofs et al.

Table 1. Observed and simulated AOT and simulated contributions from relevant modes in the dry, moist and dust periods.

	AERONET	ECHAM	ECHAM soluble		ECHAM insoluble	
	AOT	AOT	accum	coarse	accum	coarse
dry	0.183	0.132	0.124	0.006	0.000	0.000
moist	0.402	0.469	0.448	0.014	0.000	0.007
dust	0.500	0.909	0.246	0.206	0.036	0.417

[Title Page](#)
[Abstract](#)
[Introduction](#)
[Conclusions](#)
[References](#)
[Tables](#)
[Figures](#)
[I◀](#)
[▶I](#)
[◀](#)
[▶](#)
[Back](#)
[Close](#)
[Full Screen / Esc](#)
[Printer-friendly Version](#)
[Interactive Discussion](#)


**Simulation of aerosol
optical thickness
during IMPACT**

G. J. H. Roelofs et al.

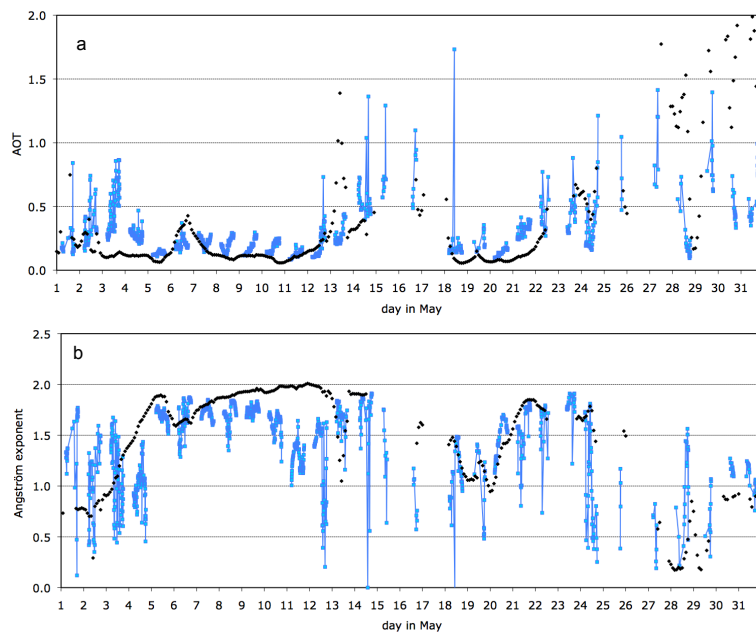


Fig. 1. Observed (blue) and simulated (black) **(a)** AOT and **(b)** Angström exponent.

[Title Page](#)[Abstract](#)[Introduction](#)[Conclusions](#)[References](#)[Tables](#)[Figures](#)[◀](#)[▶](#)[◀](#)[▶](#)[Back](#)[Close](#)[Full Screen / Esc](#)[Printer-friendly Version](#)[Interactive Discussion](#)

Simulation of aerosol optical thickness during IMPACT

G. J. H. Roelofs et al.

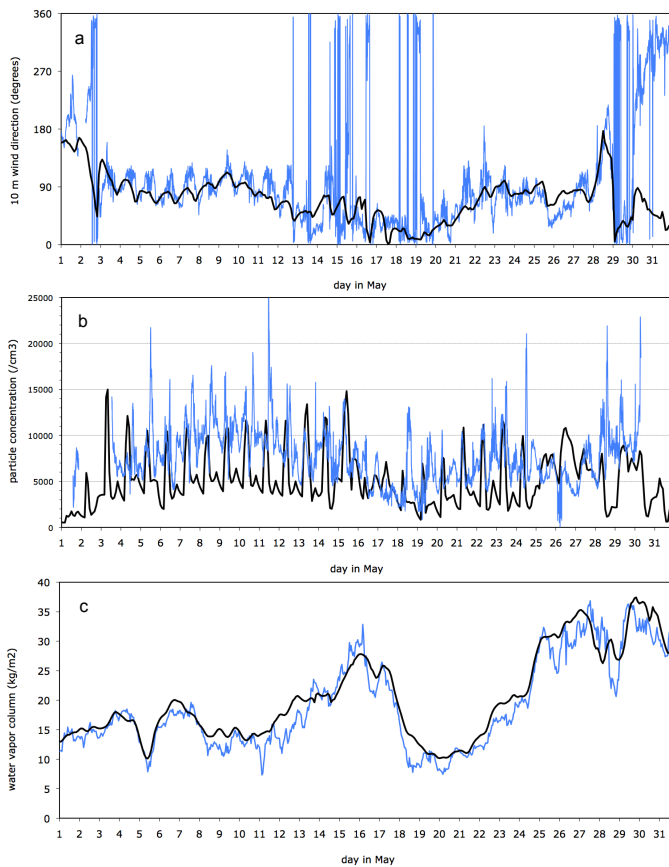


Fig. 2. Observed (blue) and simulated (black) **(a)** 10 m wind direction (degrees), **(b)** surface particle concentration (cm^{-3}), and **(c)** water vapor column (IWV, kg/m^2).

[Title Page](#)[Abstract](#)[Introduction](#)[Conclusions](#)[References](#)[Tables](#)[Figures](#)[◀](#)[▶](#)[◀](#)[▶](#)[Back](#)[Close](#)[Full Screen / Esc](#)[Printer-friendly Version](#)[Interactive Discussion](#)

Simulation of aerosol optical thickness during IMPACT

G. J. H. Roelofs et al.

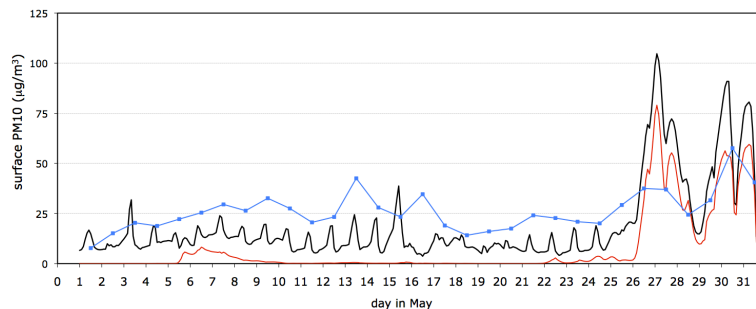


Fig. 3. Observed surface PM₁₀ (blue), and simulated aerosol (black) and dust (red) mass ($\mu\text{g}/\text{m}^3$).

[Title Page](#)[Abstract](#)[Introduction](#)[Conclusions](#)[References](#)[Tables](#)[Figures](#)[◀](#)[▶](#)[◀](#)[▶](#)[Back](#)[Close](#)[Full Screen / Esc](#)[Printer-friendly Version](#)[Interactive Discussion](#)

Simulation of aerosol
optical thickness
during IMPACT

G. J. H. Roelofs et al.

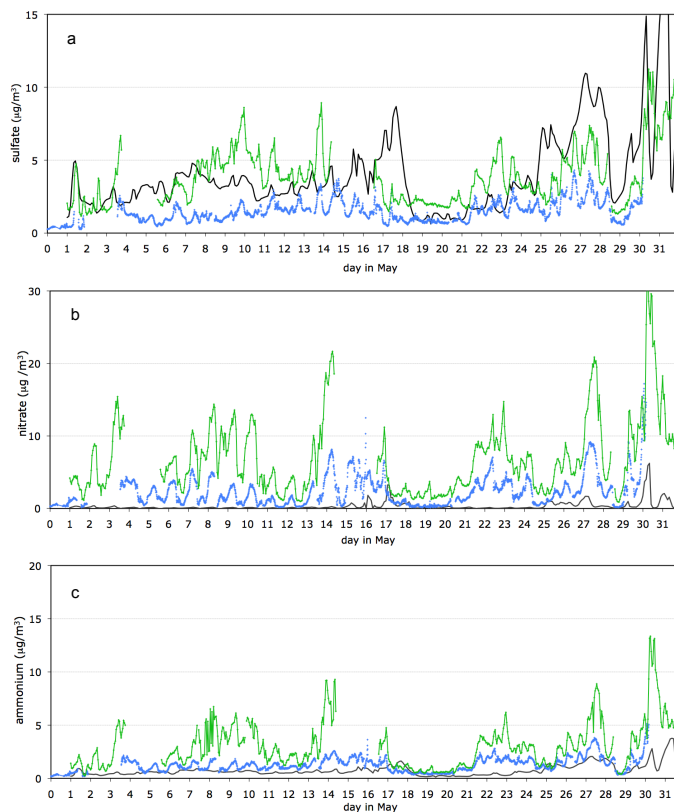


Fig. 4. Observed (blue, green) and simulated (black) concentrations ($\mu\text{g}/\text{m}^3$) of **(a)** sulfate, **(b)** nitrate, **(c)** ammonium, **(d)** organics and **(e)** chloride. Measurements in blue are from ICG-2 Jülich (Germany) and reflect particle sizes <0.56 mm diameter. Measurements in green are from ECN (The Netherlands) and reflect total aerosol mass.

Title Page

Abstract

Introduction

Conclusions

References

Tables

Figures

◀

▶

◀

▶

Back

Close

Full Screen / Esc

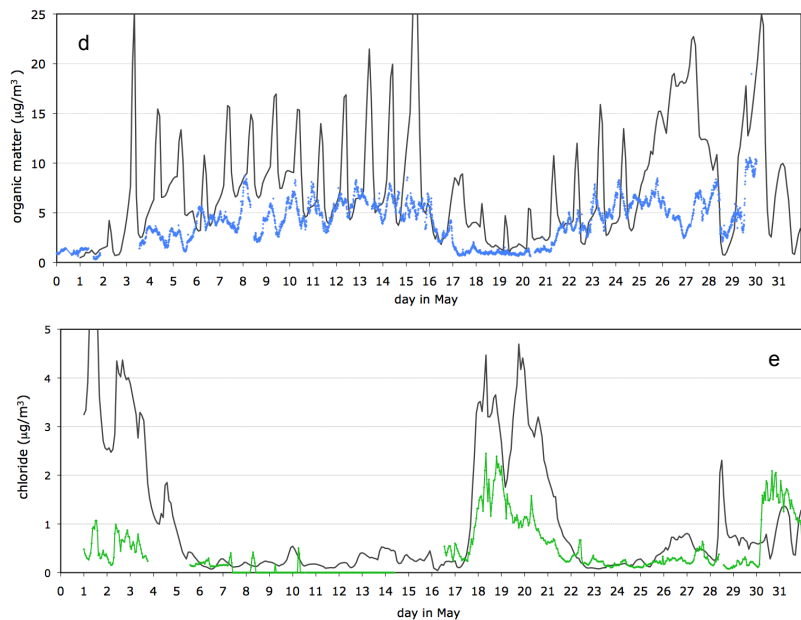
Printer-friendly Version

Interactive Discussion



**Simulation of aerosol
optical thickness
during IMPACT**

G. J. H. Roelofs et al.

**Fig. 4.** Continued.[Title Page](#)[Abstract](#)[Introduction](#)[Conclusions](#)[References](#)[Tables](#)[Figures](#)[◀](#)[▶](#)[◀](#)[▶](#)[Back](#)[Close](#)[Full Screen / Esc](#)[Printer-friendly Version](#)[Interactive Discussion](#)

Simulation of aerosol optical thickness during IMPACT

G. J. H. Roelofs et al.

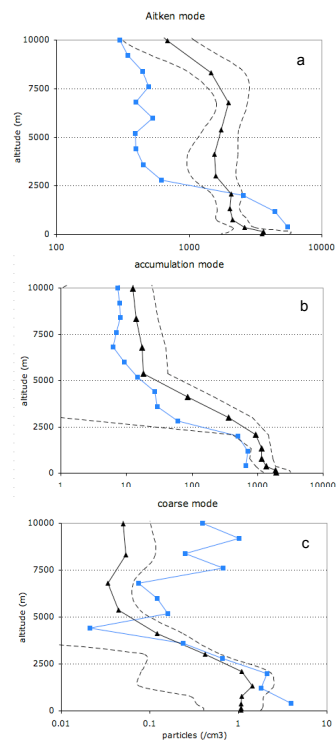


Fig. 5. Observed (blue) and simulated (black) concentration profiles (cm⁻³) averaged over 2–14 May (daytime) for **(a)** the Aitken mode (size range observations: 5–75 nm radius; model: 5–50 nm radius), **(b)** the accumulation mode (size range observations: 75–500 nm radius; model: 50–500 nm radius), and **(c)** the coarse mode (size range observations and model: >0.5 μm radius). Dashed lines reflect the simulated standard deviation.

[Title Page](#)[Abstract](#)[Introduction](#)[Conclusions](#)[References](#)[Tables](#)[Figures](#)[◀](#)[▶](#)[◀](#)[▶](#)[Back](#)[Close](#)[Full Screen / Esc](#)[Printer-friendly Version](#)[Interactive Discussion](#)

Simulation of aerosol optical thickness during IMPACT

G. J. H. Roelofs et al.

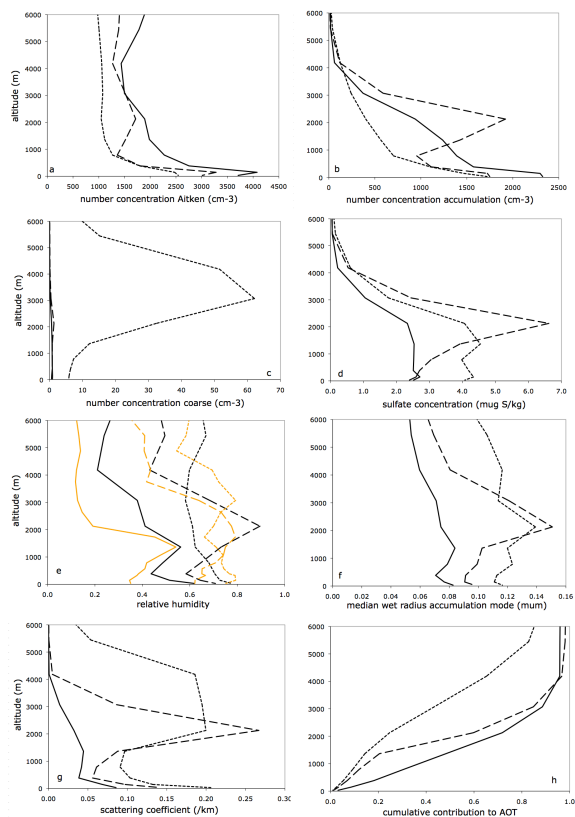


Fig. 6. Simulated profiles of number concentrations of **(a)** the Aitken, **(b)** accumulation, and **(c)** coarse mode aerosol (kg^{-1}), and of **(d)** aerosol sulfate ($\mu\text{g S kg}^{-1}$), **(e)** RH (sonde measurements in yellow), **(f)** median wet radius of the soluble accumulation mode (μm), **(g)** the scattering coefficient (km^{-1}) and **(h)** the scaled cumulative optical thickness profile, for the dry (solid line), moist (dashed) and dust periods (dotted), respectively.

Title Page

Abstract

Introduction

Conclusions

References

Tables

Figures

◀

▶

◀

▶

Back

Close

Full Screen / Esc

Printer-friendly Version

Interactive Discussion



Simulation of aerosol
optical thickness
during IMPACT

G. J. H. Roelofs et al.

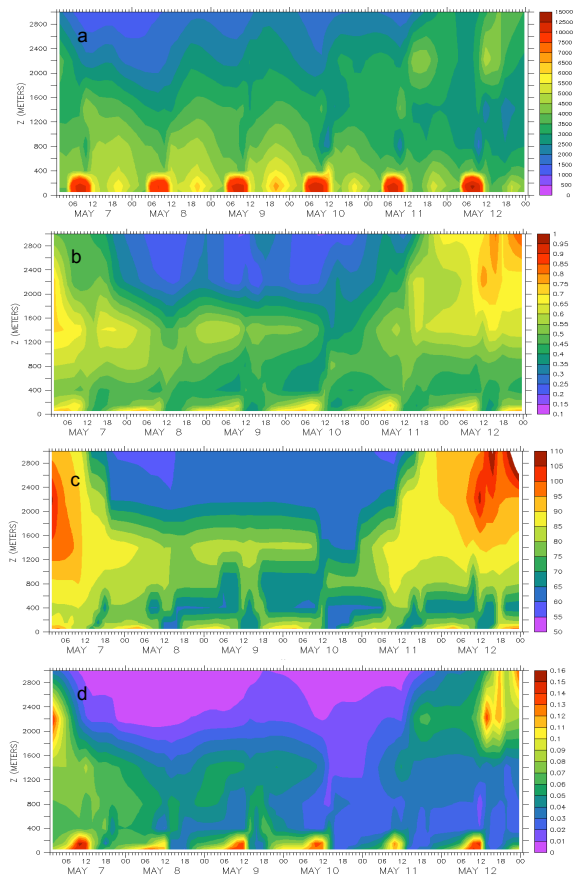


Fig. 7. (a) Fine mode particle concentration (cm^{-3}), (b) RH, (c) median wet radius of the soluble accumulation mode (nm), and (d) the scattering coefficient (km^{-1}) simulated for the dry period (7–13 May).

[Title Page](#)[Abstract](#)[Introduction](#)[Conclusions](#)[References](#)[Tables](#)[Figures](#)[◀](#)[▶](#)[◀](#)[▶](#)[Back](#)[Close](#)[Full Screen / Esc](#)[Printer-friendly Version](#)[Interactive Discussion](#)

Simulation of aerosol
optical thickness
during IMPACT

G. J. H. Roelofs et al.

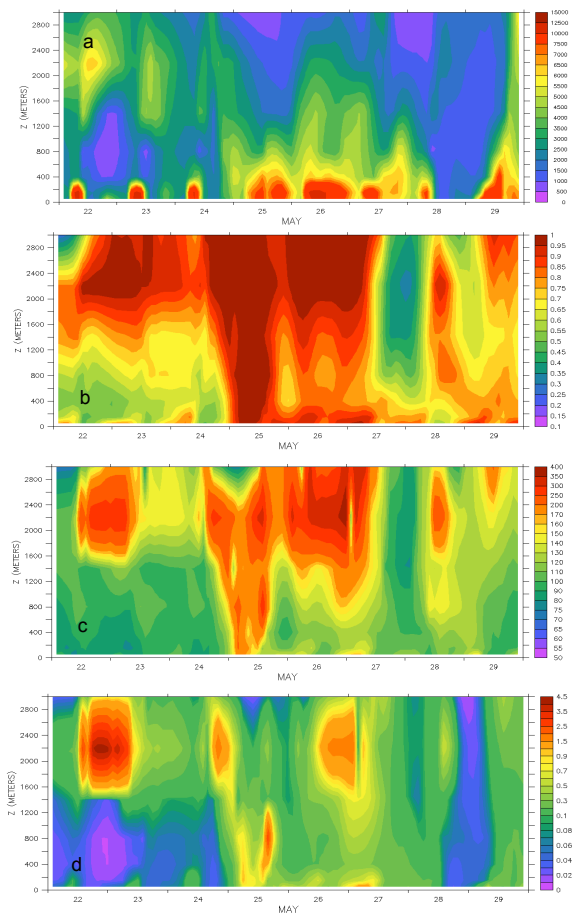


Fig. 8. (a) Fine mode particle concentration (cm^{-3}), (b) RH, (c) median wet radius of the soluble accumulation mode (nm), and (d) the scattering coefficient (km^{-1}) simulated for the moist (22–26 May) and dust periods (27–30 May).

[Title Page](#)[Abstract](#)[Introduction](#)[Conclusions](#)[References](#)[Tables](#)[Figures](#)[⏪](#)[⏩](#)[◀](#)[▶](#)[Back](#)[Close](#)[Full Screen / Esc](#)[Printer-friendly Version](#)[Interactive Discussion](#)

Simulation of aerosol
optical thickness
during IMPACT

G. J. H. Roelofs et al.

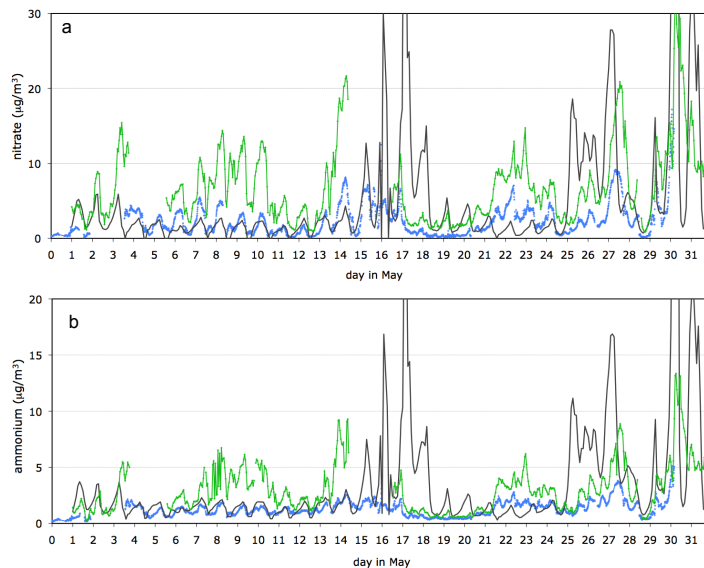


Fig. 9. Observed (blue, green; see Fig. 2) and simulated (black) concentrations ($\mu\text{g}/\text{m}^3$) of **(a)** nitrate, and **(b)** ammonium for the sensitivity study.

[Title Page](#)[Abstract](#)[Introduction](#)[Conclusions](#)[References](#)[Tables](#)[Figures](#)[◀](#)[▶](#)[◀](#)[▶](#)[Back](#)[Close](#)[Full Screen / Esc](#)[Printer-friendly Version](#)[Interactive Discussion](#)